



EFFECTS OF GEOMETRICAL ASYMMETRIES OF STRUCTURE ON DYNAMICAL CHARACTERISTICS OF TWO COUPLED CONTROL SURFACES

Y.-R. YANG

*Institute of Applied Mechanics, Southwest Jiaotong University, Chengdu 610031,
People's Republic of China*

(Received 22 August 1994, and in final form 29 May 1996)

The dynamical characteristics of two coupled control surfaces with structural asymmetries are studied. The results show that a first order and a second order perturbation method can be applied to predict free vibration frequencies and modal shapes accurately. If the stiffness value of the operational system (or asymmetrical degree) is large enough, a small asymmetrical parameter can lead to the vibration isolation of one control surface, which means that the vibrating amplitudes of one control surface are large, but those of the other control surface are close to zero. In order to avoid such vibration isolation of control surfaces, the operation stiffness (or the asymmetrical degree) must be decreased as far as possible in the structural designs of two coupled control surfaces.

© 1997 Academic Press Limited

1. INTRODUCTION

In general, the structures of all-moving tails of an aircraft or rudders of a missile are considered to be geometrically symmetrical. In engineering structures, the symmetry is often broke down by the presence of irregularity so the structures become asymmetrical. An asymmetrical structure may localize the modes of free vibration and inhibit the propagation of energy within the structure, a direct result of which is fatigue of the structure. The mode localization phenomena in the field of structural dynamics have been investigated in many research studies. In references [1–3] chains of coupled pendulums were studied, in references [4–7] multispan structures and in references [8–10] periodic structures. A common point of the models used in references [1–10] was that the models consisted of relatively simple substructures, each of which was almost identical. Recently, Natsiavas [11] studied mode localization and frequency loci veering of a new dynamical model, which was different from those used before, and its components were not similar. The above references represent only a small sample and other contributions are not listed here.

In this paper, the dynamical characteristics of two coupled control surfaces with structural asymmetries are studied by employing the first order perturbation method and the second order perturbation method, respectively. In the case of an unperturbed system with simple eigenvalues, the first order perturbation method is used to analyze the perturbed system. In the case of an unperturbed system with multiple (or dense) eigenvalues, the second order perturbation method is applied to analyze the perturbed

system. The approximate expressions for the perturbed system are used to explain roughly the reason for vibration isolation and frequency loci veering of two coupled control surfaces.

2. MODEL OF CONTROL SURFACES AND ITS VIBRATION EQUATIONS

The mechanical model of two coupled control surfaces with structural asymmetries is shown in Figure 1; this model was used as a flutter model in reference [12], but the values of parameters were a little different. In order to simplify the problem, each control surface is considered as an exactly two-degrees-of-freedom subsystem, in which h_1 (or h_2) represents the bending deformation, and α_1 (or α_2) the torsional deformation, as shown in Figure 1. The two control surfaces are coupled together by a spring with stiffness k_3 , which represents the operation stiffness coefficient. So, the undamped free vibration equation of the control surfaces are

$$M\ddot{\xi} + K\xi = 0, \quad (1)$$

where

$$M = \begin{bmatrix} m_1 & (1-x_0)m_1 & 0 & 0 & 0 \\ (1-x_0)m_1 & I_1 + (1-x_0)^2 b_r^2 m_1 & 0 & 0 & 0 \\ 0 & 0 & I_0/r_1^2 & 0 & 0 \\ 0 & 0 & 0 & I_2 + (1-x_0)^2 b_r^2 m_2 & (1-x_0)b_r m_2 \\ 0 & 0 & 0 & (1-x_0)b_r m_2 & m_2 \end{bmatrix},$$

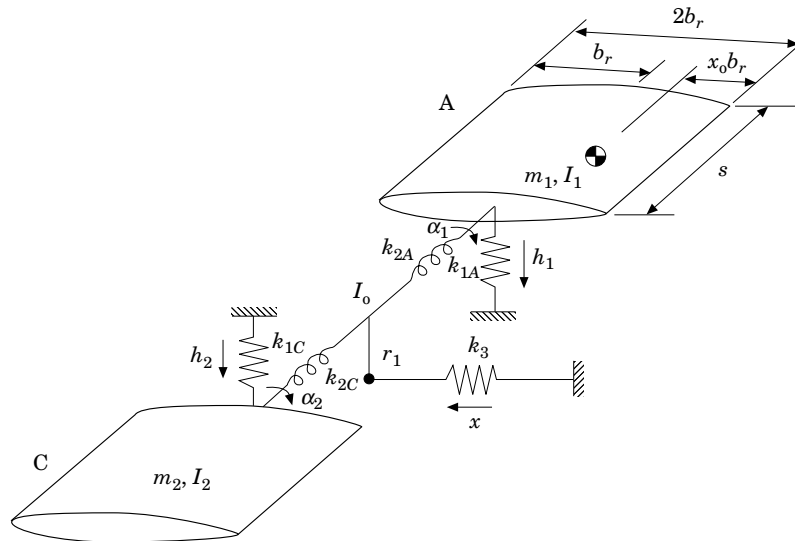


Figure 1. Sketch of mechanical model of two coupled control surfaces. h_1 and h_2 denote bending deformations of the two control surfaces separately, α_1 and α_2 represent torsion deformations of two control surfaces separately, x is the deformation of the operation system, k_{1A} , k_{2A} , m_1 and I_1 are the bending stiffness coefficient, the torsional stiffness coefficient, the mass and the inertial moment of control surface A respectively, k_{1C} , k_{2C} , m_2 and I_2 are the bending stiffness coefficient, the torsional stiffness coefficient, the mass and the inertial moment of control surface C respectively, and k_3 is the stiffness coefficient of the operation system.

$$K = \begin{bmatrix} k_{1A} & 0 & 0 & 0 & 0 \\ 0 & k_{2A} & -k_{2A}/r_1 & 0 & 0 \\ 0 & -k_{2A}/r_1 & k_3 + (k_{2A} + k_{2C})/r_1^2 & -k_{2C}/r_1 & 0 \\ 0 & 0 & -k_{2C}/r_1 & k_{2C} & 0 \\ 0 & 0 & 0 & 0 & k_{1C} \end{bmatrix},$$

$$\xi = \{h_1 \quad \alpha_1 \quad x \quad \alpha_2 \quad h_2\}, \quad \ddot{\xi} = d^2\xi/dt^2, \quad t \text{ is time.}$$

Generally speaking, the parameter I_0 is small and k_3 large in equation (1). In order to introduce a small parameter, Guyan's method [13] is used to reduce equation (1) and the corresponding non-dimensional equation can be expressed in the form

$$M_1 d^2\zeta/d\tau^2 + (K_0 + cK_1)\zeta = 0 \quad (2)$$

where

$$\zeta = \{\tilde{h}_1 \quad \alpha_1 \quad \alpha_2 \quad \tilde{h}_2\}.$$

$$M_1 = \begin{bmatrix} 1 & (1-x_0) & 0 & 0 \\ (1-x_0) & I & 0 & 0 \\ 0 & 0 & \mu I & \mu(1-x_0) \\ 0 & 0 & \mu(1-x_0) & \mu \end{bmatrix},$$

$$K_0 = \begin{bmatrix} 1 & 0 & 0 & 0 \\ 0 & \omega_A^2 & 0 & 0 \\ 0 & 0 & \mu\rho_2^2\omega_A^2 & 0 \\ 0 & 0 & 0 & \mu\rho_1^2 \end{bmatrix},$$

$$K_1 = \begin{bmatrix} 0 & 0 & 0 & 0 \\ 0 & -(\omega_A^2 b_r/r_1)^2 & -\mu(\rho_2\omega_A^2 b_r/r_1)^2 & 0 \\ 0 & -\mu(\rho_2\omega_A^2 b_r/r_1)^2 & -(\mu\rho_2^2\omega_A^2 b_r/r_1)^2 & 0 \\ 0 & 0 & 0 & 0 \end{bmatrix}, \quad c = \frac{k_{1A}}{k_3 + (k_{2A} + k_{2C})/r_1},$$

$$\tau = \sqrt{k_{1A}/m_1}, \quad I = (L/b_r)^2 + (1-x_0)^2, \quad L^2 = I_1/m_1 = I_2/m_2,$$

$$\mu = m_2/m_1, \quad \tilde{h}_1 = h_1/b_r, \quad \tilde{h}_2 = h_2/b_r, \quad \rho_1^2 = k_{1C}m_1/k_{1A}m_2,$$

$$\rho_2^2 = k_{2C}m_1/k_{2A}m_2, \quad \omega_A^2 = k_{2A}/k_{1A}b_r^2.$$

In a practical structure, $k_3 \gg k_{1A}$, so the value of c (see equation (3)) is small and can be considered as a small parameter. Obviously, when $\mu = \rho_1^2 = \rho_2^2 = 1$, the two coupled control surfaces become symmetrical. Generally speaking, among the three parameters, only $\mu \neq 1$ means that the mass of the structure is asymmetrical; only $\rho_1^2 \neq 1$ means that the bending stiffness of structure is asymmetrical; only $\rho_2^2 \neq 1$ means that the torsional stiffness of the structure is asymmetrical.

3. SIMPLE DESCRIPTION OF THE SMALL PARAMETER EXPANSION METHOD

Here, two cases are considered. The first case is that the unperturbed system has simple eigenvalues and each eigenvalue is not close to any other one. The first order perturbation

method is used to analyze the perturbed system in this case. The second case is that the unperturbed system has multiple eigenvalues or highly dense eigenvalues. The second order perturbation method must be used to analyze the perturbed system in this case.

3.1. UNPERTURBED SYSTEM WITH SIMPLE EIGENVALUES

The eigenproblem corresponding to equation (2) is

$$((K_0 + cK_1) - \lambda M_1)y = 0, \quad (4)$$

where $\lambda = \omega^2$, ω is the frequency and y is the eigenvector.

The power series expansions of eigenvalues and eigenvectors are

$$\lambda = \lambda|_{c=0} + \lambda'c + O(c^2), \quad y = y|_{c=0} + y'c + O(c^2). \quad (5, 6)$$

The determinant corresponding to equation (4) is

$$\|(K_0 + cK_1) - \lambda M_1\| = 0. \quad (7)$$

When $c = 0$, the eigenvalues of equation (7) are

$$\lambda_{1,3} = \frac{1}{2}(b_r/L)^2[I + \omega_A^2 \pm \sqrt{(I + \omega_A^2)^2 - 4(L\omega_A/b_r)^2}], \quad (8, 9)$$

$$\lambda_{2,4} = \frac{1}{2}(b_r/L)^2[\rho_1^2 I + \rho_2^2 \omega_A^2 \pm \sqrt{(\rho_1^2 I + \rho_2^2 I)^2 - 4(L\rho_1\rho_2\omega_A/b_r)^2}]. \quad (10, 11)$$

That is, $\lambda|_{c=0} = \lambda_i$, $i = 1, 2, 3, 4$. The normalized eigenvectors corresponding to λ_i , ($i = 1, 2, 3, 4$), are

$$\psi_i = (1/\sqrt{e_i})\{(1 - x_0)\lambda_i \quad (1 - \lambda_i) \quad 0 \quad 0\}, \quad i = 1, 3, \quad (12)$$

$$\psi_j = (1/\sqrt{e_j})\{0 \quad 0 \quad (\rho_1 - \lambda_j) \quad (1 - x_0)\lambda_j\}, \quad j = 2, 4, \quad (13)$$

where

$$e_i = (L(1 - \lambda_i)/b_r)^2 + (1 - x_0)^2, \quad e_j = \mu \left(\frac{L(\rho_1 - \lambda_j)}{b_r} \right)^2 + \mu\rho_1^4(1 - x_0)^2;$$

that is, $y|_{c=0} = \psi_k$, $k = 1, 2, 3, 4$.

According to reference [14], the eigenvalues and eigenvectors of the first-order perturbation expansions have the expressions

$$\lambda_{app}^{(i)} = \lambda_i + \lambda'_i c, \quad y_{app}^{(i)} = \psi_i + y'_i c, \quad i = 1, 2, 3, 4, \quad (14, 15)$$

where

$$\lambda'_i = \psi_i^T K_1 \psi_i, \quad y'_i = \sum_{j=1}^4 \eta_{ji} \psi_j, \quad \eta_{ji} = \frac{\psi_j^T K_1 \psi_i}{\lambda_i - \lambda_j}, \quad j \neq i, \quad \eta_{ii} = 0. \quad (16-19)$$

3.2. UNPERTURBED SYSTEM WITH MULTIPLE (OR DENSE) EIGENVALUES

In the model used here, when $\mu = \rho_1 = \rho_2 = 1$, the unperturbed system has two double eigenvalues; when the value of μ , ρ_1 and ρ_2 are in the vicinity of 1, the eigenvalues of the unperturbed system have the following properties: the first eigenvalue is close to the second one; the third one is close to the fourth one. So, the second order terms must be considered.

The technique of the small parameter method for multiple eigenvalues is different from that for simple eigenvalues [15]. Here, the method described in reference [16] is used to solve for the eigenvalues and the eigenvectors. Let

$$y_i = \phi_1 q_i, \quad i = 1, 2, \quad y_j = \phi_2 q_j, \quad j = 3, 4, \quad (20, 21)$$

where $\phi_1 = [\psi_1 \ \psi_2]$, $\phi_2 = [\psi_3 \ \psi_4]$, ψ_i is expressed in equations (12) and (13) and q_i and q_j are constant vectors.

Substituting equations (20, 21) into equation (4) and pre-multiplying it by ϕ_1^T or ϕ_2^T respectively, one can obtain the expressions

$$\phi_1^T(K_0 + cK_1)\phi_1 q_i = \mu_i \phi_1^T M_1 \phi_1 q_i, \quad j = 1, 2, \quad (22)$$

$$\phi_2^T(K_0 + cK_1)\phi_2 q_j = \mu_j \phi_2^T M_1 \phi_2 q_j, \quad j = 3, 4. \quad (23)$$

According to Rayleigh's principle, if $\phi_1 q_i$ differs from the eigenvector of the perturbed system by a small quantity of first order in c , μ_i differs from the eigenvalue of the perturbed system by a small quantity of second order in c . μ_i , q_i , μ_j and q_j can be solved using equations (22) and (23) respectively.

So, for the first two eigenvalues and eigenvectors, one may assume

$$\lambda_{app}^{(i)} = \mu_i + \lambda_{i2} c^2 + O(c^3), \quad y_{app}^{(i)} = \phi_1 q_i + y_{i1} c + y_{i2} c^2 + O(c^3), \quad i = 1, 2, \quad (24, 25)$$

where $y_{im} \perp \phi_i q_i$ (or ϕ_1), $m = 1, 2$. One can now substitute equations (24) and (25) into equation (4). If the concept of a progressive approach is used, one can obtain expressions

$$(K_0 - \mu_i M_1)\phi_1 q_i + c[K_1 \phi_1 q_i + (K_0 - \mu_i M_1)y_{i1}] = 0, \quad (26)$$

$$c^2[(K_0 - \mu_i M_1)y_{i2} + K_1 y_{i1} - \lambda_{i2} M_1 \phi_1 q_i] = 0. \quad (27)$$

Because of the conditions of normalization, $y_{im} \perp \phi_1$ ($m = 1, 2$), the expression y_{im} can be assumed in the form

$$y_{im} = \eta_{3m} \psi_3 + \eta_{4m} \psi_4, \quad m = 1, 2. \quad (28)$$

Substituting equation (28) into equation (26) pre-multiplying it by ψ_m^T , $m = 3, 4$, respectively, one can conclude

$$y_{i1} = \sum_{m=3}^4 \frac{\psi_m^T K_1 \phi_1 q_i}{\mu_i - \lambda_m} \psi_m, \quad i = 1, 2. \quad (29)$$

Pre-multiplying equation (27) by ψ_m^T , $m = 3, 4$ and $q_i^T \phi_i^T$ respectively, one can conclude

$$y_{i2} = \sum_{m=3}^4 \frac{\psi_m^T K_1 y_{i1}}{\mu_i - \lambda_m} \psi_m, \quad \lambda_{i2} = \frac{q_i^T \phi_1^T K_1 y_{i1}}{q_i^T q_i}, \quad i = 1, 2. \quad (30, 31)$$

Using the above-mentioned steps for the last two eigenvalues and eigenvectors, one can obtain the similar expressions

$$\lambda_{app}^{(j)} = \mu_j + \lambda_{j2} c^2 + O(c^3), \quad y_{app}^{(j)} = \phi_2 q_j + y_{j1} c + y_{j2} c^2 + O(c^3), \quad j = 3, 4, \quad (32, 33)$$

where

$$y_{j1} = \sum_{m=1}^2 \frac{\psi_m^T K_1 \phi_2 q_j}{\mu_j - \lambda_m} \psi_m, \quad y_{j2} = \sum_{m=3}^4 \frac{\psi_m^T K_1 y_{j1}}{\mu_j - \lambda_m} \psi_m, \quad \lambda_{j2} = \frac{q_j^T \phi_2^T K_1 y_{j1}}{q_j^T q_j}, \quad j = 3, 4. \quad (34)$$

4. FREE VIBRATION ANALYSIS

The values of the parameters in Figure 1 are taken to be $m_1 = m_2 = 4.545$ kg, $I_0 = 0.0549$ kg m², $I_1 = I_2 = 0.2984$ kg m², $r_1 = 0.0762$ m, $b_r = s = 0.254$ m, $x = 0.2$,

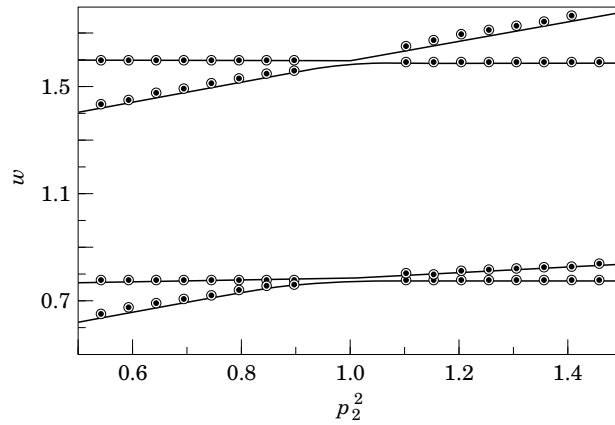


Figure 2. The curves of the first frequency and the second frequency versus ρ_2^2 . $\rho_1^2 = 1$, $c = 0.00146$. The solid line represents the exact solutions, dots the values given by the first order perturbation, 'O' the values given by the second order perturbation.

$k_{1A} = 70.04$ kN/m, $k_{2A} = 7.23$ kN m/rad, $k_3 = 45.45$ MN/m. So, the values of normalized parameters are $\mu = 1$, $I = 1.6576$, $\omega_A^2 = 1.6$ and $c = 0.00146$.

4.1. EFFECTS OF ASYMMETRICAL PARAMETERS ON FREQUENCIES

When $\rho_1^2 = 1$, the changes of natural frequency ω with the parameter ρ_2^2 are shown in Figure 2 and Table 1. In Figure 2, the real lines represent the exact solutions, the dots the computational values from equation (14) and 'o' the values from equation (24). When $\rho_2^2 = 1$ (symmetrical parameters), two double-eigenvalues can be obtained if one uses equations (14). The exact solutions show that no double-eigenvalue appears, but the first frequency is close to the second one and the third one close to the fourth one, as shown in Table 1. The calculated values from equations (24) and (32) can simulate the tendency of the exact solutions. This is to say, with the first order perturbation method, the veering of the eigenvalue loci can be mistaken for a crossing; whereas the second order perturbation method can obtain the curve veering of the eigenvalue loci.

TABLE 1
The changes of frequencies versus ρ_2^2 , for $|1 - \rho_2^2| \leq 0.05$

ρ_2^2	ω_1			ω_2			ω_3			ω_4		
	A*	B*	C*	A	B	C	A	B	C	A	B	C
0.95	0.745	0.760	0.760	0.745	0.776	0.775	1.59	1.58	1.58	1.61	1.61	1.60
0.96	0.747	0.762	0.762	0.747	0.776	0.776	1.59	1.58	1.58	1.61	1.61	1.61
0.97	0.749	0.764	0.764	0.749	0.777	0.776	1.60	1.58	1.58	1.61	1.61	1.61
0.98	0.751	0.765	0.765	0.751	0.778	0.777	1.60	1.59	1.59	1.61	1.61	1.61
0.99	0.753	0.766	0.766	0.753	0.778	0.777	1.61	1.59	1.59	1.61	1.61	1.61
1.00	0.755	0.767	0.768	0.755	0.779	0.778	1.61	1.59	1.59	1.61	1.61	1.61
1.01	0.755	0.768	0.768	0.757	0.780	0.779	1.61	1.59	1.59	1.61	1.61	1.61
1.02	0.755	0.769	0.769	0.759	0.782	0.781	1.61	1.59	1.59	1.62	1.62	1.62
1.03	0.755	0.769	0.770	0.761	0.783	0.782	1.61	1.59	1.59	1.62	1.62	1.62
1.04	0.755	0.770	0.770	0.763	0.784	0.783	1.61	1.60	1.60	1.62	1.62	1.62
1.05	0.755	0.770	0.770	0.764	0.786	0.785	1.61	1.60	1.60	1.63	1.62	1.62

*A is the results of the first order perturbation method; B is the results of the second order perturbation method; C is the exact solution.

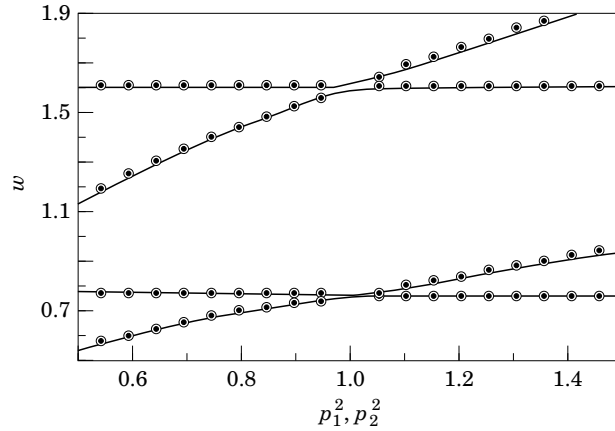


Figure 3. The curves of the first frequency and the second frequency versus ρ_1^2 or ρ_2^2 . $\rho_1^2 = \rho_2^2$, $c = 0.00146$. Key as Figure 2.

When $\rho_2^2 = 1$, the changes of ω with the parameter ρ_1^2 are almost the same as those shown in Figure 2. Now, however, another special case is analyzed, that when $\rho_1^2 = \rho_2^2$. The changes of ω with ρ_1^2 or ρ_2^2 are shown in Figure 3, in which the symbols are the same as those in Figure 2. It is obvious that the tendencies of the variation shown in Figure 2 and Figure 3 are similar.

From Figure 2 and Table 1, it is obvious that there are no differences in principle between the values of the first order perturbation and those of the second order perturbation when $|1 - \rho_2^2| > 0.05$.

4.2. EFFECTS OF ASYMMETRICAL PARAMETERS ON MODAL SHAPES

Here, only the case of $\rho_1^2 = 1$ is considered. A number of calculated results show that the other cases are similar to this case.

When $|1 - \rho_2^2| > 0.05$, the curves of the ratio \tilde{h}_1/\tilde{h}_2 versus ρ_2^2 are shown in Figure 4, in which the solid lines represent the exact solutions, the dots the approximate solutions of equation (15) and 'o' the values from equation (25). Only the ratios of the first mode and the second mode are depicted in Figure 4. The calculated results show that the tendency

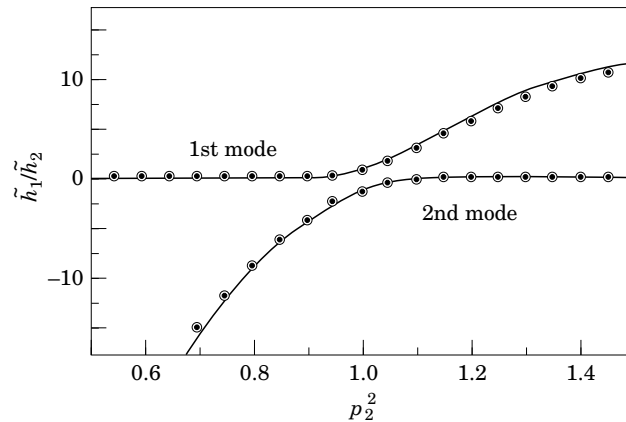


Figure 4. The curves of \tilde{h}_1/\tilde{h}_2 versus ρ_2^2 for the first mode and second mode. $\rho_1^2 = 1$, $c = 0.00146$, $|1 - \rho_2^2| > 0.05$. Key as Figure 2.

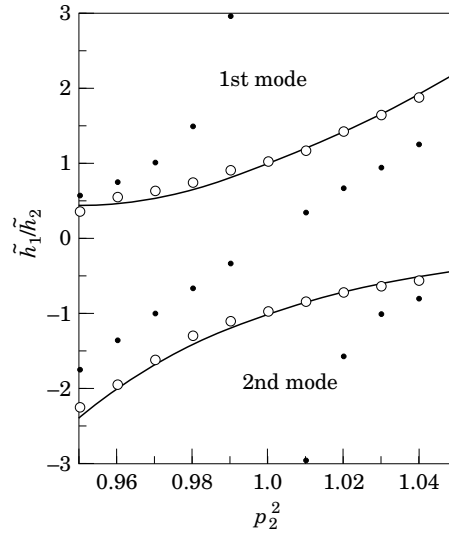


Figure 5. The curves of \tilde{h}_1/\tilde{h}_2 versus ρ_2^2 for the first mode and second mode. $\rho_1^2 = 1$, $c = 0.00146$, $|1 - \rho_2^2| < 0.05$. Key as Figure 2.

of the variation of the third mode is similar to that of the first mode, and that of the fourth mode is similar to that of the second mode. On the other hand, the tendency of the variation of the ratio α_1/α_2 is similar to that of the ratio \tilde{h}_1/\tilde{h}_2 for the values of the parameters given above. So, the basic tendency of the variation of each mode of the structure may be represented by Figure 4, which shows that strong vibration isolation happens for much wider values of the parameter. The concept of vibration isolation means that certain modes may become highly localized, and associated with the bending (or the torsion) displacements of control surface A (see Figure 1) or with those of control surface C. In Figure 4, it is obvious that the degree of vibration isolation depends on the value of the difference $|1 - \rho_2^2|$: the larger the absolute value, the higher is the degree of vibration isolation.

When $|1 - \rho_2^2| < 0.05$, the curves of the ratio \tilde{h}_1/\tilde{h}_2 versus ρ_2^2 are shown in Figure 5, in which the symbols are the same as those in Figure 4. This condition belongs to the case of the unperturbed system with multiple (or dense) eigenvalues (see Table 1). From Figure 5, one can see that the values of the second order perturbation agree with those of the exact solutions, but the first order perturbation method is invalid.

4.3. EFFECTS OF PARAMETER c (OR k_3) ON MODAL SHAPES

First, the case of $c \rightarrow 0$ (or $k_3 \rightarrow \infty$) is discussed. In this case, because the second part and the third part of the right sides of equations (25) and (33) are equal to zero, the approximate solutions are equal to the exact solutions. From the point of view of a practical structure, the control surfaces A and C become decoupled. From equations (12, 13, 25, 33), the vibration isolation is typical. That is the ratio \tilde{h}_1/\tilde{h}_2 (or α_1/α_2) of each mode equals either infinity or zero.

Secondly, the case of $c > 0$ is examined. When c is very small, the first part of the right sides of equations (25) and (33) plays a dominant role in the approximate expression for the modal shapes, which means that the properties of the modal shapes of the perturbed system are similar to those of the unperturbed system. Figure 4 shows a set of typical results. But when c is not very small, the first part of the right sides does not play a

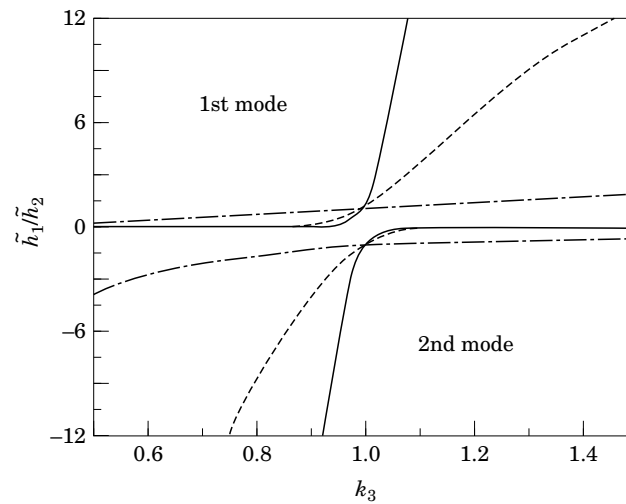


Figure 6. The curves of \tilde{h}_1/\tilde{h}_2 versus k_3 for the first mode and second mode. $\rho_1^2 = 1$. Solid line denotes the values when $k_3 = 200$ MN/m, dashed line the values when $k_3 = 45.45$ MN/m, — · — the values when $k_3 = 4.545$ MN/m.

dominant role in equations (25) and (33) and the roles of the second part and the third part of the right sides increase. So, there is the possibility that no mode becomes localized. Figure 6 shows the curves of changes of the first mode, the second mode with parameter c , which shows that no vibration isolation is observed when $k_3 = 4.545$ MN/m, unless the value of ρ_2^2 is very large. One can conclude that the parameter c plays an important role in the vibration isolation of the control surfaces with structural asymmetries. A similar conclusion for the mode localization of multispan beams can be found in reference [6]. Equations (25) and (33) show that if one of the modes is localized, the others will be localized.

5. CONCLUSIONS

One asymmetrical parameter contained in the two coupled control surfaces may induce vibration isolation of the structure; so do many parameters.

The degree of vibration isolation of the coupled control surfaces depends on the coupling parameter c and the values of $|1 - \rho_i^2|$, $i = 1, 2$. The larger the values of k_3 ($= 1/c$) and $|1 - \rho_i^2|$, $i = 1, 2$, the higher is the degree of vibration isolation. If the stiffness value of the operational system is large enough, a small asymmetrical parameter can lead to vibration isolation. In order to avoid the vibration isolation of two coupled control surfaces, the operation stiffness (or the asymmetrical degree) must be decreased as far as possible in the structural design of two coupled control surfaces.

From the preliminary analysis, if one of the modes of the control surfaces with structural asymmetries is localized, all the modes are localized. The second order perturbation method can be used to calculate approximately the strong vibration isolation of the examined structure to good accuracy.

REFERENCES

1. C. H. HODGES 1982 *Journal of Sound and Vibration* **82**, 411–424. Confinement of vibration by structural irregularity.

2. C. H. HODGES and J. WOODHOUSE 1983 *Journal of the Acoustical Society of America* **74**, 894–905. Vibration isolation from irregularity in a nearly periodic structure: theory and measurements.
3. G. S. HAPPAWANA, A. K. BAJAJ and O. D. I. NWOKAH 1991 *Journal of Sound and Vibration* **147**, 361–365. A singular perturbation perspective on mode localization.
4. C. PIERRE 1988 *Journal of Sound and Vibration* **126**, 485–502. Mode localization and eigenvalue loci veering phenomena in disordered structures.
5. C. PIERRE and E. H. DOWELL 1987 *Journal of Sound and Vibration* **114**, 549–564. Localization of vibrations by structural irregularity.
6. C. PIERRE, D. M. TANG and E. H. DOWELL 1987 *American Institute of Aeronautics and Astronautics Journal* **25**, 1249–1257. Localization vibrations of disordered multispan beams: theory and experiment.
7. S. D. LUST, P. P. FRIEDMAN and O. O. BENDIKSON 1990 *American Institute of Aeronautics and Astronautics Journal* **28**, 225–235. Mode localization in multispan beams.
8. O. O. BENDIKSEN 1987 *American Institute of Aeronautics and Astronautics Journal* **25**, 1241–1248. Mode localization phenomena in large space structures.
9. D. J. EWINS and Z. S. HAN 1984 *Journal of Vibration, Acoustics, Stress and Reliability in Design* **106**, 211–215. Resonant vibration levels of a mistuned bladed disk.
10. P. J. CORNWELL and O. O. BENDIKSEN 1989 *American Institute of Aeronautics and Astronautics Journal* **27**, 219–226. Localization of vibrations in large space reflectors.
11. S. NATSIAVAS 1993 *Journal of Sound and Vibration* **165**, 137–147. Mode localization and frequency veering in a non-conservative mechanical system with dissimilar components.
12. C. LEE 1986 *American Institute of Aeronautics and Astronautics Journal* **24**, 833–840. An iterative procedure for nonlinear flutter analysis.
13. R. J. GUYAN 1965 *American Institute of Aeronautics and Astronautics Journal* **3**, 380. Reduction of stiffness and matrices.
14. L. MEIROVITCH 1980 *Computational Methods in Structural Dynamics*. The Netherlands: Sijthoff & Noordhoff International Publisher B.V.
15. R. COURANT and D. HILBERT 1953 *Methods of Mathematical Physics* (Vol. 1). New York: Interscience.
16. J. K. LIU and X. M. ZHANG 1995 *Journal of Northwestern Polytechnical University* (in Chinese) **13**, 336–339. A new perturbation method for general eigenvalue problem.